Iron toxicity resistance strategies in tropical grasses: The role of apoplastic radicular barriers

Advanio Inácio Siqueira-Silva[1,3,], Camilla Oliveira Rios[2], Eduardo Gusmão Pereira[1]*

1. *Institute of Biological and Health Sciences, Federal University of Viçosa (UFV), Campus Florestal, Florestal, Minas Gerais, Brazil*
2. *Postgradute Program in Management and Conservation of Natural and Agrarian Ecosystems, UFV Campus Florestal, Florestal, Minas Gerais, Brazil*
3. *Federal University of Western Pará (UFOPA), University Campus of Juruti, Juruti, Pará, Brazil*

ARTICLE INFO

ABSTRACT

The revegetation of mined areas poses a great challenge to the iron ore mining industry. The initial recovery process in degraded areas might rely on the use of Fe-resistant grasses. Tropical grasses, such as *Paspalum densum* and *Echinochloa crus-galli*, show different resistance strategies to iron toxicity; however, these mechanisms are poorly understood. The Fe-resistance mechanisms and direct iron toxicity as a function of root apex removal were investigated. To achieve this purpose, both grass species were grown for up to 480 hr in a nutrient solution containing 0.019 or 7 mmol/L Fe-EDTA after the root apices had been removed or maintained. Cultivation in the presence of excess iron-induced leaf bronzing and the formation of iron plaque on the root surfaces of both grass species, but was more significant on those plants whose root apex had been removed. Iron accumulation was higher in the roots, but reached phytotoxic levels in the aerial parts as well. It did not hinder the biosynthesis of chloroplastidic pigments. No significant changes in gas exchange and chlorophyll *a* fluorescence occurred in either grass when their roots were kept intact; the contrary was true for plants with excised root apices. In both studied grasses, the root apoplastic barriers had an important function in the restriction of iron translocation from the root to the aerial plant parts, especially in *E. crus-galli*. Root apex removal negatively influenced the iron toxicity resistance mechanisms (tolerance in *P. densum* and avoidance in *E. crus-galli*).

© 2018 The Research Center for Eco-Environmental Sciences, Chinese Academy of Sciences. Published by Elsevier B.V.

Introduction

Iron (Fe) is an essential mineral element for plant growth and development (Celletti et al., 2016; Jucoski et al., 2013; Müller et al., 2017), and participates in enzyme-catalyzed processes, such as nitrogen fixation; DNA, hormone, and chloroplast synthesis; and the maintenance of photosynthesis and respiration (Briat et al., 2015). However, an excess of Fe in foliar tissues (above 500 mg/kg dry mass) can induce toxicity in most plant species (Broadley et al., 2012; Pugh et al., 2002). Iron phytotoxicity can be direct (absorption of the metal with accumulation in plant tissues) (Lobréaux et al., 1995; Schmidt, 2006) or indirect (Fe plaque formation on the root surface, which affects nutrient absorption by the plant) (Araújo et al., 2014; Siqueira-Silva et al., 2012; Zhang et al., 1999). Iron toxicity is a complex phenomenon that can affect different

---

morphological, physiological, and biochemical aspects of plants, such as photosynthesis, cellular structural integrity, nutritional composition, chloroplastidic pigmentation, polyphenol content, reactive oxygen species production, and oxidative stress induction (Müller et al., 2015, 2017).

A correct selection of plant species is paramount to successful conservation and recovery programs in environments degraded by mining activities. Generally, Fe-resistant species (Rios et al., 2017) that are capable of surviving and regenerating at the site of interest should be included (de la Fuente et al., 2014). *Paspalum densum* (Poir.) and *Echinochloa crus-galli* (L.) P. Beauv. are tropical plants of the Poaceae family that exhibit Fe-resistance strategies (Rios et al., 2017). However, the mechanisms that confer resistance and allow them to grow in the presence of high Fe concentrations are not well-studied. Therefore, this gap in information should be filled to pursue the goal of ensuring the success of their use in revegetating mining areas, as well as to investigate new Fe-resistant species. Plants can resist Fe toxicity through mechanisms such as avoidance and tolerance (Zhang et al., 2016); these mechanisms are respectively based on the restriction of absorption and formation of iron plaque on the root surface (Deng et al., 2010; Li et al., 2017) and cellular compartmentalization (Müller et al., 2015), or the neutralization and removal of reactive oxygen species, metal chelation, and detoxification (Michalak, 2006; Sytar et al., 2013). In most roots, the apoplastic (intercellular spaces and cell walls) movement of solute and water across the root cortex to the xylem is blocked by the Casparian strip (Zhan et al., 2018), an integral band-like portion of the wall and intercellular substance that is impregnated with suberin and sometimes lignin (Evert, 2006). The presence of apoplastic barriers that exhibit Casparian strips, such as the endodermis and the exodermis, contribute to the avoidance strategy, and can decrease metal-induced phytotoxicity by preventing the assimilation of metals within the roots, and consequently hindering their translocation and accumulation in the aerial parts (Redjala et al., 2011; Silva et al., 2013; Tylová et al., 2017) and protecting the plant from stress (Yousefi et al., 2018). Apoplastic barriers are characterized by their hydrophobicity (Redjala et al., 2011), and were reported to be effective barriers to prevent the movement of heavy metals (Al, Cd, Hg) into the stele (Huang et al., 2018; Silva et al., 2013; Wang et al., 2015). However, the roles of apoplastic barriers in Fe uptake and translocation in Fe-resistant tropical grasses are still unclear. The direct effect of excess Fe in these plants can be observed by the mechanical removal of root apices, and consequently the elimination of the apoplastic barriers imposed by the endodermis and/or exodermis. The employed resistance strategies vary among plant species and depend on the duration and intensity of exposure to the metal (Rios et al., 2017).

In this context, the present study hypothesizes that two grass species, *P. densum and E. crus-galli*, exhibit different resistance strategies when grown in the presence of excess Fe. The objective of the present study was thus to identify the mechanisms involved in Fe-resistance and to evaluate the direct effects of Fe toxicity. The results found may be useful in the selection of plant species resistant to Fe toxicity, and in greater understanding the metal tolerance mechanisms.

1. Materials and methods

1.1. Experimental growth conditions and treatments

The experiments were conducted in a greenhouse (19°53′20.23″S, 44°25′56.38″W) in a hydroponic system, using the tropical grasses *Paspalum densum* (Poir.) and *Echinochloa crus-galli* (L.) P. Beauv., both of which are members of the Poaceae family. Seeds of both species were obtained from mining areas of the Iron Quadrangle region in the state of Minas Gerais, Brazil, and sowed in a sand bed. After emergence, healthy and homogenous seedlings were transplanted into 5-L polypropylene pots (5 seedlings/pot) containing Hoagland nutrient solution (Hoagland and Arnon, 1950) at ½ strength (pH 5.0) without aeration. Seedlings remained under hydroponic conditions for 30 days; after which they were acclimated to a full strength solution as a function of their development and nutritional requirements. The acclimation process continued for 112 days, during which *P. densum* and *E. crus-galli* were pruned two and three times, respectively, at a stem height of 4 cm for homogenization; the nutrient solution was renewed every 7 days and the pH was measured and adjusted every 2 days using NaOH and HCl, as required. After acclimation, half of the plants from each treatment had 10 cm of the root apex excised using a surgical blade. At 10 cm from the root apex, the endoderm of both grass species was completely differentiated near the region of maturation. The root cutting exposed the central cylinder and consequently allowed the elimination of the apoplastic barrier imposed by the endoderm. Root segments with similar length (40 cm) were cut together to ensure standardization of the removed root region. Due to the heterogeneity of root lengths, not all the root apices were excised. Root removal was performed in nutrient solution to prevent xylem cell cavitation. Subsequently, both grasses (with intact or excised roots) were grown in different iron concentrations (0.019 (control), and 7 mmol/L Fe-EDTA) for 0, 12, 120, 240, and 480 hr. During this period, the pH was measured daily, and the nutrient solution was renewed weekly; its volume was supplemented with deionized water whenever necessary.

1.2. Iron content in plants

The Fe content in the shoots and roots of both the grass species was determined after 0, 12, 120, 240, and 480 hr of cultivation under the control (with normal iron content) or excess iron concentrations, following methodology proposed by Tedesco et al. (1995). Briefly, the dried and crushed plant material was digested in nitrate-perchlorate solution (3:1, *V/V*), and the iron content in the extract thus obtained was quantified by atomic absorption spectrophotometry (GBC Avanta, GBC Scientific Equipment, Australia). Roots were washed with dithionite–citrate–bicarbonate (DCB) to remove iron and other mineral elements adhered to the root surface in the form of plaque (Liu et al., 2008).

1.3. Evaluation of chlorophyll indices

The chloroplast pigment indices (total chlorophyll, chlorophyll *a*, chlorophyll *b*, and chlorophyll *a/b* ratio) were estimated during the experiments using a ClorofiLOG portable meter (CFL1030, Falker, Brazil). The measurements were performed on the same leaves that were used in fluorescence and gas exchange analysis.

1.4. Gas exchange measurements

The gas exchange variables: Photosynthesis rate (A); stomatal conductance (g_s); transpiration (E); and the ratio of internal and external CO_2 concentrations (C_i/C_a), were measured between 08:00 a.m. and 12:00 p.m. for all treatments with plants grown in control or excess Fe. An infrared gas analyzer – IRGA (LI-6400XT, LI-COR Biosciences, USA), equipped with a radiation source of 1500 mol/(m^2·sec) and a CO_2 concentration of 400 µmol/mol, was used for the measurements, which were performed on completely expanded and apparently healthy leaves; these leaves were mostly the second and third leaves of *E. crus-galli* and *P. densum*, respectively.

1.5. Chlorophyll *a* fluorescence analysis

The chlorophyll *a* fluorescence variables were determined using a Mini-PAM modulated pulse fluorometer (Heinz Walz, Germany), after 0, 12, 120, 240, and 480 hr of treatment exposure. The measurements were carried out during the morning (8:00 a.m.–12:00 p.m.) on the same leaves where the gas exchange analyses were performed. After dark-acclimation of the leaves for at least 60 min, the minimum (F_0) and maximum (F_m) fluorescence values were recorded. These values were used to calculate the maximum quantum yield of photosystem II: $F_v/fm = (F_m-F_0)/F_m$ (Genty et al., 1989). The plant tissue was subsequently subjected to photosynthetically active radiation (PAR) for 60 s with an intensity of 1000 µmol/(m^2·sec). After this period, a saturating actinic light pulse was applied to determine the following parameters: F_s, steady-state fluorescence; F_m, maximum fluorescence in light-acclimated plant tissue; $\phi_{PSII} = (F_{m'}-F_s)/fm'$, effective quantum yield of the photochemical energy conversion in photosystem II (Genty et al., 1989); $\phi_{NPQ} = (F_s/fm')-(F_s/fm)$, quantum yield of regulated energy dissipation; $\phi_{NO} = F_s/fm$, quantum yield of non-regulated energy dissipation (Hendrickson et al., 2004); $qL = (F_{m'}-F_s)/(F_{m'}-F_{0'}) \times F_{0'}/F_s$, photochemical quenching (Kramer et al., 2004); $NPQ = (F_m-F_{m'})/fm'$, non-photochemical quenching (Bilger and Björkman, 1990); and $ETR = \phi_{II} \times PAR \times 0.84 \times 0.5$, apparent electron transport rate, where 0.84 was the value that corresponded to the fraction of light that was absorbed by the leaves, and 0.5 corresponded to the fraction of excited energy distributed in the photosystem II (Melis et al., 1987). The minimum fluorescence values of light-adapted samples ($F_{0'}$) were calculated using the approximation $F_{0'} = F_0/(F_v/F_m + F_0/F_{m'})$ introduced by (Oxborough and Baker, 1997).

1.6. Assessment of hydrogen peroxide (H_2O_2) contents

Hydrogen peroxide (H_2O_2) levels were determined in all treatments with different exposure times using the same leaves on which gas exchange was analyzed; this was done according to the methodology proposed by Velikova et al. (2000).

1.7. Assessment of malonaldehyde (MDA) content

The MDA contents were determined in all samples and control at the different times outlined before and that were exposed to control or excess iron concentrations; the determination was done using leaves that were used for chlorophyll *a* fluorescence analysis previously, according to the methodology proposed by Hodges et al. (1999).

1.8. Experimental design and statistical analyses

The experimental design was based on a random block design in a factorial scheme with two plant species (*P. densum* and *E. crus-galli*), two concentrations of iron (0.019 and 7 mmol/L Fe-EDTA), two types of roots (intact and excised), and five exposure times (0, 12, 120, 240, and 480 hr). Four replicates were established per treatment. Data obtained from each collection was submitted to two-way analysis of variance and regression with mean values compared by Tukey's test at a 5% probability level using SAEG 9.2-UFV software (Fundação Arthur Bernardes, UFV, Viçosa, Brazil).

2. Results

2.1. Phytotoxic effects of Fe on the external morphology of roots and leaves

When cultivated in excess iron concentrations, both grass species exhibited the formation of an iron plaque on the intact or excised root surface and foliar bronzing. These symptoms became more evident after 12 hr and intensified after 96 hr of exposure to Fe-EDTA. Bronzing was more intense in fully expanded leaves and in specimens with excised roots. The color of iron plaque differed between the two species: orange in *E. crus-galli* and grayish in *P. densum*.

After 240 hr of cultivation of both species in a nutrient solution with excess Fe, the treatment of plants with excised roots was interrupted due to the observation of symptoms of toxicity and imminent death.

2.2. Iron concentration in the aerial part and roots

The Fe content in the aerial parts of both species reached values above phytotoxic levels: 693 and 920 mg/kg dry matter in *E. crus-galli* and *P. densum*, respectively, when these grasses had their root apex excised and were exposed to excess iron (Fig. 1a, b). The root was the main vegetative organ for Fe accumulation in both species. However, in *E. crus-galli*, this value was approximately 11-fold higher than that in *P. densum* (Fig. 1c, d). The state of the roots influenced the mineral absorption that plants could effectively perform in the
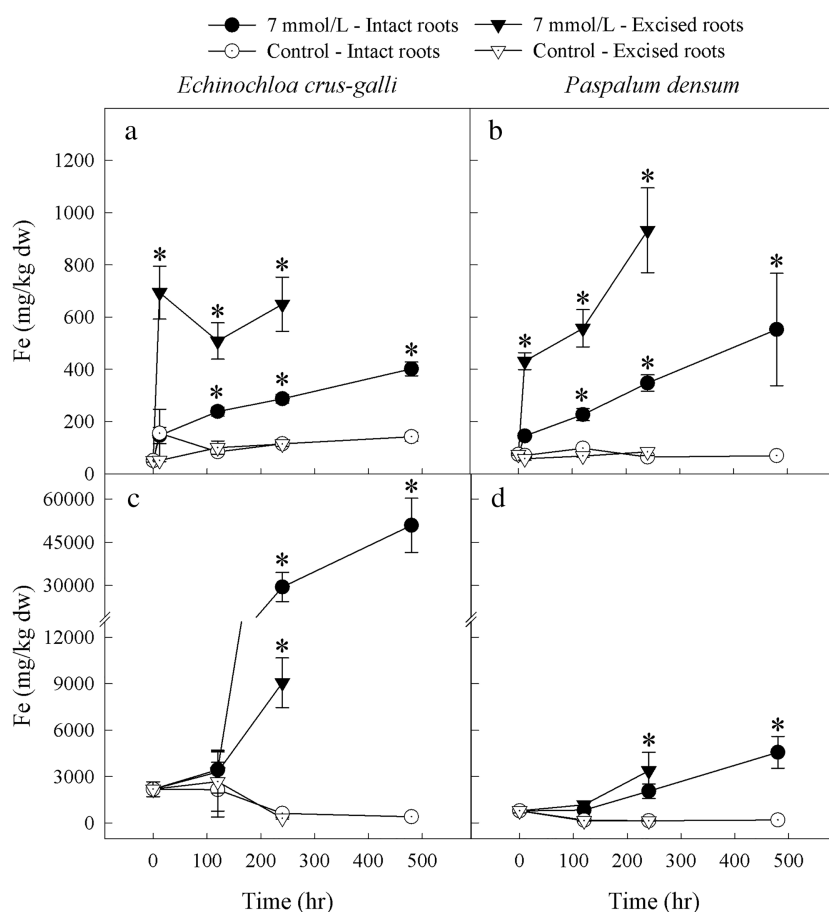
Fig. 1 – Iron content in aerial parts (a and b) and roots (c and d) of *Echinochloa crus-galli* (a and c) and *Paspalum densum* (b and d) after cultivation for 0, 12, 120, 240, and 480 hr at concentrations of 0.019 and 7 mmol/L Fe-EDTA and with two root morphological types (intact and excised). Bars represent the mean ± standard error of four replicates. Asterisks (*) indicate significant difference by Tukey's test at 5% significance. dw: dry weight.

presence of excess iron: *E. crus-galli* plants with intact roots exhibited the highest iron content after 240 hr of treatment. *P. densum* also exhibited the highest Fe content in its roots (excised or intact) after 240 hr, when exposed to excess iron conditions (Fig. 1c, d).

2.3. Effect of excess iron on chloroplastidic pigments

In relation to photosynthetic pigments (total chlorophyll, chlorophyll *a*, chlorophyll *b*, and chlorophyll *a/b* ratio), there was no significant difference between the applied treatments, regardless of the exposure time, root morphology, and iron concentration in the nutrient solution; there was no significant difference between the evaluated species either (Appendix A Fig. S1).

2.4. Phytotoxic effects of excess Fe on leaf gas exchange

In both grasses, the lowest photosynthetic rates (A) were observed in plants with excised roots exposed to excess Fe (Fig. 2a, b). This decrease was observed after 12 and 240 hr for *P. densum* and *E. crus-galli*, respectively. The net

photosynthetic rate was also significantly lower in both species when their roots were intact, after 480 hr of exposure to excess iron, when compared with that of control plants (Fig. 2a, b).

Transpiration (*E*) was significantly reduced after 120 and 240 hr in either *P. densum* or *E. crus-galli*, respectively, when their roots were excised and they were grown in excess iron (Fig. 2c, d). The lowest *E* in both the species were observed when they were grown in the presence of excess iron after 480 hr of cultivation (Fig. 2c, d).

A significant reduction in stomatal conductance (g_s) was observed in *E. crus-galli* and *P. densum* after 480 hr of exposure to excess iron when their roots were kept intact, compared to that of the respective control group (Fig. 2e, f). *P. densum* plants with excised roots presented significantly lower g_s values when grown in excess iron after 12 hr of exposure (Fig. 2f).

A significant increase of the C_i/C_a ratio in *E. crus-galli* was observed after 480 hr in plants with intact roots cultivated in the presence of excess Fe compared to that in the control (Fig. 2g). The highest C_i/C_a values in *P. densum* were observed in plants with excised roots cultivated in excess Fe after 12 hr of exposure (Fig. 2h).
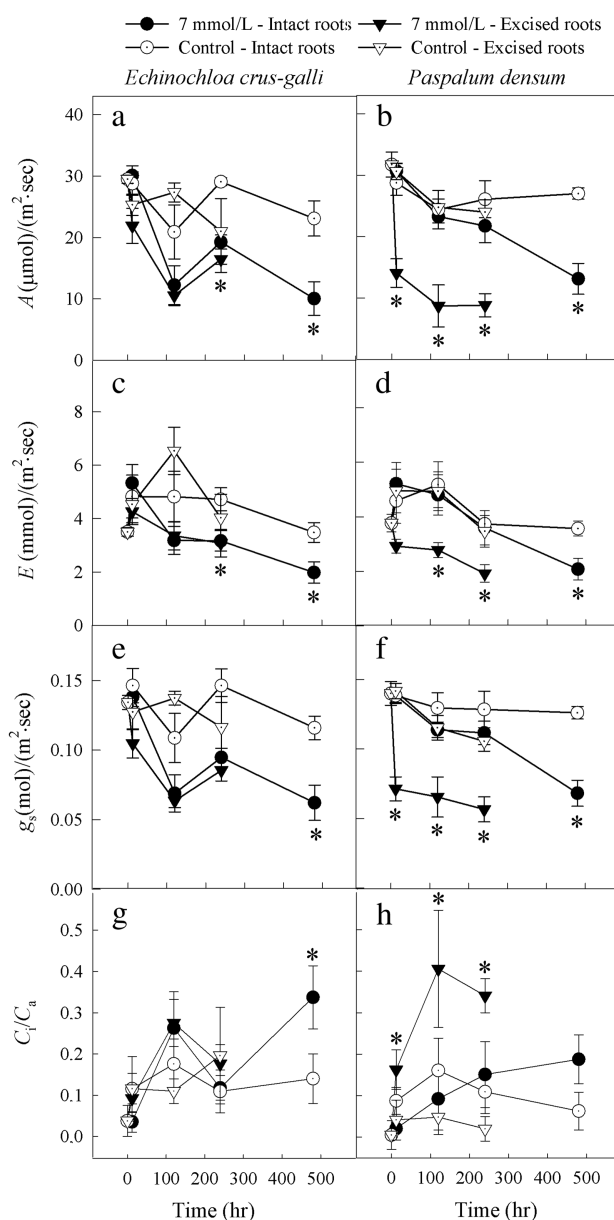
Fig. 2 – Variations in photosynthetic rates (A) (a and b), transpiration (E) (c and d), stomatal conductance (g_s) (e and f), and internal and external CO_2 concentration ratios C_i/C_a (g and h) for *Echinochloa crus-galli* (a, c, e, and g) and *Paspalum densum* (b, d, f, and h) after cultivation for 0, 12, 120, 240, and 480 hr at concentrations of 0.019 and 7 mmol/L Fe-EDTA, and with two root morphological types (intact and excised). Bars represent the mean ± standard error of four replicates. Asterisks (*) indicate significant differences by Tukey's test at 5% significance.

2.5. Chlorophyll *a* fluorescence response to iron toxicity

The minimum fluorescence (F_0) and the maximum quantum yield of photosystem II (F_v/fm) in *E. crus-galli* did not present significant differences between the different treatments (morphological root types and exposure to Fe toxicity) (Fig. 3a, c). *P. densum* with excised roots and treated with 7 mmol/L Fe-EDTA presented significantly higher F_0 and lower F_v/fm values, which differed from all other treatments after 120 hr of exposure (Fig. 3b, d).

The electron transport rate (ETR) in *E. crus-galli* was similar among the different treatments and exposure times (Appendix A Fig. S2). After 120 hr of exposure to excess Fe, the ETR values in *P. densum* with excised roots decreased; they differed significantly from the other treatments. The photochemical (qL) and NPQ in both grasses did not vary with the treatments and exposure times (Appendix A Fig. S2).

The excision of the root apex and the concentration of iron in the nutrient solution did not interfere with the effective quantum yield of photosystem II (ϕ_{PSII}) in *E. crus-galli*, regardless of the length of exposure to excess iron (Fig. 4a). After 120 hr of exposure, this variable had decreased significantly in *P. densum* cultivated in excess Fe and with excised roots (Fig. 4b). The quantum yield of regulated energy
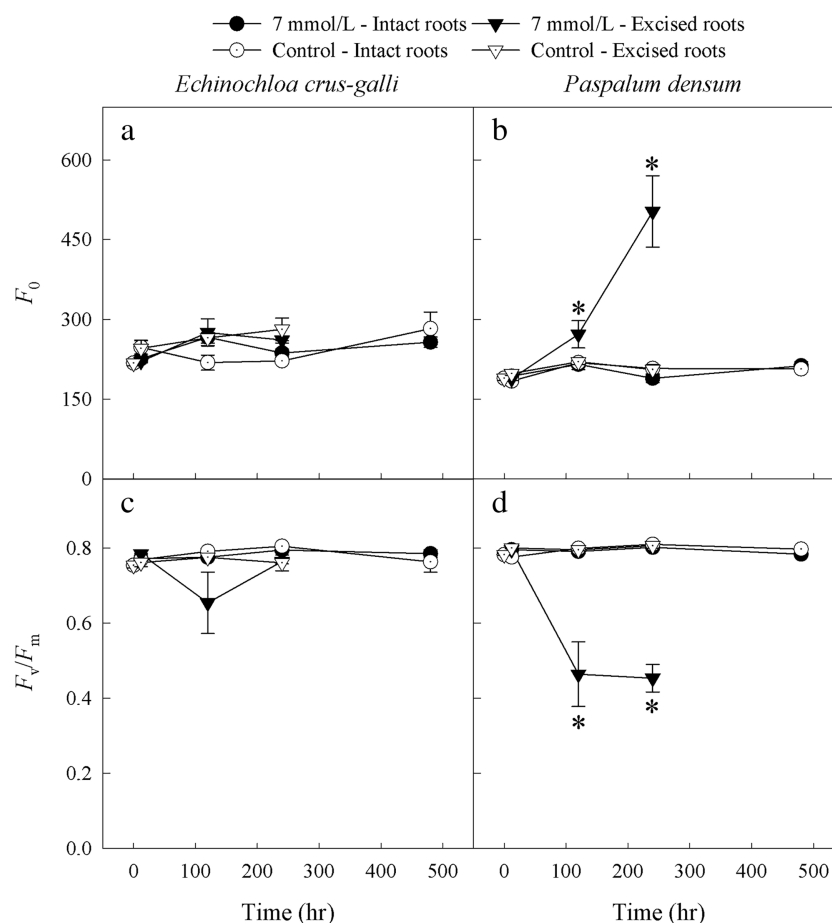
Fig. 3 – Fluorescence minimum (F_0) (a and b) and photosystem II maximum quantum yield (F_v/fm) (c and d) for grasses, _Echinochloa crus-galli_ (a and c) and _Paspalum densum_ (b and d), after cultivation for 0, 12, 120, 240, and 480 hr at concentrations of 0.019 and 7 mmol/L Fe-EDTA and with two root morphological types (intact and excised). Bars represent the mean ± standard errors of four replicates. Asterisks (*) indicate significant difference by Tukey's test at 5% significance.

dissipation in PSII (ϕ_{NPQ}) in both species did not vary significantly among the different treatments and with the exposure times (Fig. 4c, d). However, the non-regulated quantum yield of energy dissipation in PSII (ϕ_{NO}) showed a significant difference between the treatments for 12 and 120 hr in both _E. crus-galli_ and _P. densum_, respectively, with a reduction in ϕ_{NO} for the former and an increase for the latter (Fig. 4e, f).

2.6. Hydrogen peroxide contents and lipid peroxidation

The foliar H_2O_2 contents showed no variation among the different treatments and with the exposure times in _E. crus-galli_ (Fig. 5a). At the maximum exposure time to excess Fe (480 hr), _P. densum_ with intact roots showed a significant H_2O_2 increase as compared to the control (Fig. 5b).

The foliar malonaldehyde (MDA) content remained constant between plants from the different treatments and exposure times, except at 120 and 240 hr in _E. crus-galli_ and _P. densum_, respectively, whose specimens cultivated under excess iron conditions and with excised roots exhibited a significant increase (Fig. 5c, d).

3. Discussion

Intensification in the absorption and consequent accumulation of Fe in the aerial parts of _E. crus-galli_ and _P. densum_ after excision of their roots is attributable to the free translocation of the metal towards the stem and leaves. During the short-term exposure to iron excess (_E. crus-galli_, 12 hr and _P. densum_, 120 hr), Fe metal accumulation surpassed phytotoxic levels (>500 mg/kg dry mass of leaves) (Broadley et al., 2012; Pugh et al., 2002). A greater accumulation of Fe in roots, as seen in _E. crus-galli_ in response to Fe toxicity, may be a strategy to avoid translocation of the metal to the aerial parts. This has previously been reported in Fe-resistant grasses, such as _Setaria parviflora_ and _Paspalum urvillei_ (Araújo et al., 2014; Santana et al., 2014). Despite the fact that the apoplastic barriers could be modified depending on nutrient availabilities (Barberon et al., 2016; Doblas et al., 2017), the presence of this anatomical structure in the intact roots of both grasses studied here restricted the iron uptake, such as observed for other metals and in other plant species (Lyubenova et al., 2012; Yamaguchi et al., 2011). Elimination of the apoplastic
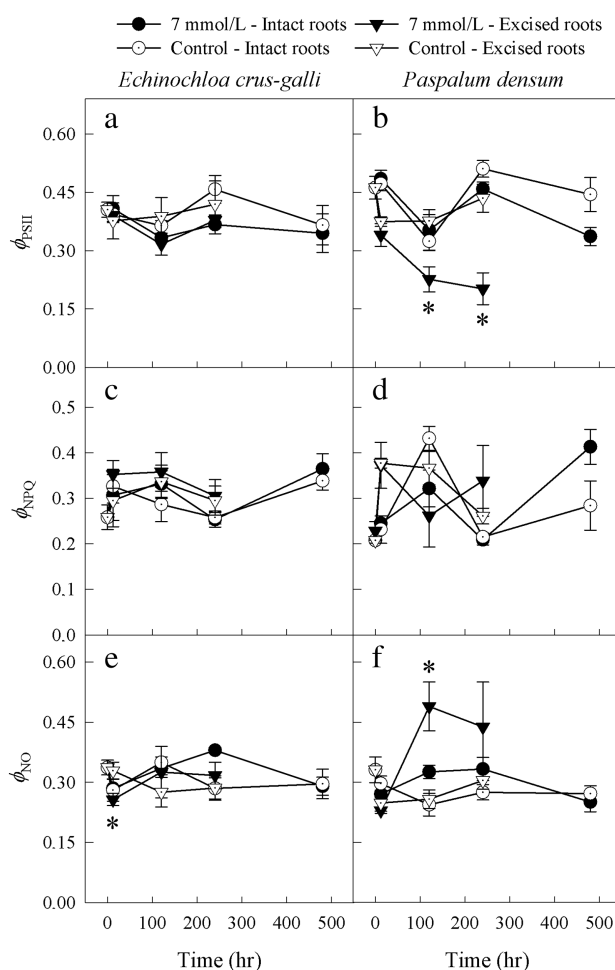
Fig. 4 – Effective quantum efficiency of photochemical energy conversion in photosystem II (φ_{PSII}) (a and b), regulated energy dissipation quantum yield (φ_{NPQ}) (c and d), and non-regulated energy dissipation quantum yield (φ_{NO}) (e and f) for grasses, *Echinochloa crus-galli* (a, c, and e) and *Paspalum densum* (b, d, and f), after cultivation for 0, 12, 120, 240, and 480 hr at concentrations of 0.019 and 7 mmol/L Fe-EDTA and with two root morphological types (intact and excised). Bars represent the mean ± standard error of four replicates. Asterisks (*) indicate significant difference by Tukey's test at 5% significance.

barrier (endoderm) by removal of the apices and other portions of the roots allowed a greater translocation of iron towards the aerial parts of *E. crus-galli*, a non-Fe-accumulating tropical grass, and increased the effects induced by Fe toxicity in both the species.

The formation of Fe plaques on the root surface, which is considered to be an effective barrier against phytotoxic metals by many authors (Deng et al., 2010; Li et al., 2017; Sebastian and Prasad, 2016; Wu et al., 2017), may have contributed to the reduction of Fe uptake in the grasses investigated here; this can be considered a metal exclusion strategy. Heavy metal tolerance mechanisms are not always restricted to the root system, and can be also related to the shoots (Silva et al., 2013). Reduced Fe retention in root tissues, and thus, greater translocation of the metal to the aerial parts of *P. densum* may constitute a tolerance-based strategy (rather than avoidance) against iron accumulation. The results prove the existence of metal resistance mechanisms in plants with intact roots; these are the mechanisms that operate outside the endoderm and prevent metal translocation to the aerial

parts (Silva et al., 2013) while maintaining iron homeostasis in plants.

Leaf bronzing, as observed in *E. crus-galli* and *P. densum*, is a typical symptom of direct Fe toxicity that occurs due to its accumulation in the plant tissues and damage to the cellular components (Becker and Asch, 2005; Pinto et al., 2016; Santana et al., 2014; Wu et al., 2014). The highest intensity of this foliar injury in plants with excised roots arises from the fact that more Fe was absorbed and translocated to the aerial parts, therefore making the plant more prone to Fe toxicity-induced damage.

Iron is essential for chlorophyll biosynthesis (Broadley et al., 2012). The maintenance of chloroplast pigment contents, as seen by the equilibrium in their biosynthesis and breakdown among the plants from different treatments of excess and normal iron concentrations and over time, was an indicator of both Fe-resistance and an absence of oxidative stress in both species.

Generally, no significant physiological damage to the photosynthetic apparatus of either species was observed;
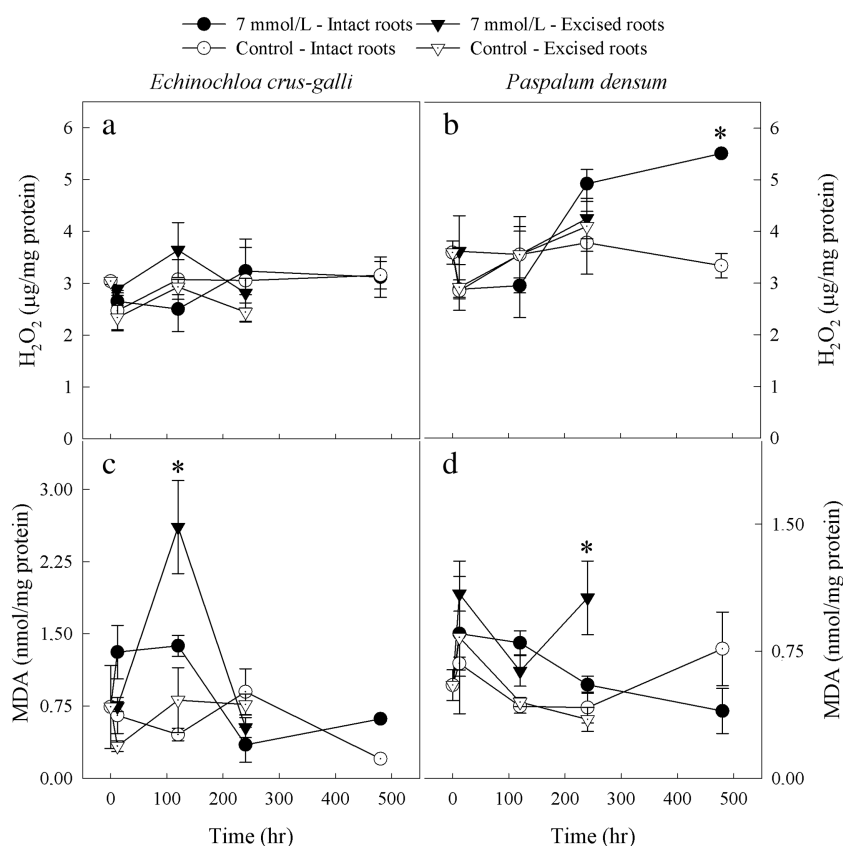
Fig. 5 – H$_2$O$_2$ (a and b) and malonaldehyde (MDA) (c and d) concentrations in *Echinochloa crus-galli* (a and c) and *Paspalum densum* (b and d) leaves after cultivation for 0, 12, 120, 240, and 480 hr at concentrations of 0.019 and 7 mmol/L Fe-EDTA and with two root morphological types (intact and excised). Bars represent the mean ± standard error of four replicates. Asterisks (*) indicate significant difference by Tukey's test at 5% significance.

moreover, there was no evidence of oxidative damage, another indicator of Fe-resistance (Pinto et al., 2016). Variations in gas exchange when grown under excess Fe, as reported here for *E. crus-galli* and *P. densum*, are typical symptoms of iron toxicity in other plant species (Adamski et al., 2011; Silva et al., 2015; Xu et al., 2015). These variations may have been enhanced in the present study by the removal of the root apices, which increases Fe absorption and translocation. The decrease in the photosynthetic rate, transpiration, and stomatal conductance, and increase in the C_i/C_a ratio, indicated that Fe-induced non-stomatal limitations occurred in both species. The decrease in the quantum yield of photosystem II and the apparent electron translocation rate in *P. densum* in the present study confirms the onset of photoinhibition (Murata et al., 2007) induced by the excision of the root apices and cultivation under excess Fe conditions. The increase in F_0 values in *P. densum* under the two stress conditions (root excision and excess Fe) indicates either damage to the photosystem II reaction center or a reduction in the excitation energy transfer capacity from the antenna complex to the reaction centers (Yuan et al., 2013); these alterations may have contributed to the decrease in photosynthetic variables in plants subjected to this treatment.

The maintenance of non-regulated energy dissipation quantum yield values (ϕ_{NO}) under excess iron conditions in both grasses throughout the duration of the experiment indicated the ability of the species to dissipate excess energy by regulating their photochemistry or by other regulatory protection mechanisms. NPQ, which is an important mechanism in plants that protects their reaction centers of photosystem II from damage through the dissipation of energy as heat (Pinto et al., 2016), was also not altered in both species, regardless of the treatment and length of exposure to toxic Fe concentrations.

Exposure to high concentrations of Fe may induce the production of ROS, including H$_2$O$_2$. ROS are highly toxic to plant cells and require detoxification (Adamski et al., 2012; Kobayashi and Nishizawa, 2012; Pinto et al., 2016). Although high foliar H$_2$O$_2$ levels were found in *P. densum* specimens with intact roots that were cultivated for 480 hr under excess iron conditions, this ROS was efficiently detoxified without membrane degradation, as indicated by the low concentration of the lipid peroxidation byproduct, MDA. Membrane lipids are reliable indicators of oxidative stress in plants (Halliwell, 1987); they were not affected in either grass species studied here, as can be seen in the low MDA concentrations in all treatments, except for those with root apex removal and cultivation with excess Fe. However, in *E. crus-galli*, a physiological adjustment was observed that led to a decrease in MDA concentration, shortly after it reached the peak of its

production. The same trend for this parameter was not observed in *P. densum*. Low MDA values were indicative of resistance to iron toxicity and the fact that the plants possessed an internal ROS control mechanism.

The methodology of root apex removal and differential Fe accumulation in the roots and aerial parts of the studied species demonstrated the different Fe toxicity resistance mechanisms in them. In *E. crus-galli,* an avoidance strategy was observed with a high metal accumulation in its roots; in *P. densum,* a tolerance strategy was adopted with high iron concentrations observed in its aerial parts. The two species studied have root apoplastic barriers with important functions in the restriction of iron translocation from the root to the aerial plant parts, especially *E. crus-galli*.

4. Conclusions

Root apex removal negatively influenced the Fe toxicity resistance mechanisms in the studied tropical grasses (tolerance and avoidance mechanisms in *P. densum* and *E. crus-galli*, respectively). The phytotoxic effect of iron and the consequent strategy adopted for metal resistance were more evident when the roots of the both species had been excised, proving the efficiency of this method and the importance of apoplastic barriers at preventing the assimilation of Fe within the roots, and consequently, hindering their translocation to, and accumulation in, the aerial parts of the plants.

Acknowledgments

Appendix A. Supplementary data.

Supplementary data to this article can be found online at https://doi.org/10.1016/j.jes.2018.10.005.

REFERENCES

Adamski, J.M., Peters, J.A., Danieloski, R., Bacarin, M.A., 2011. Excess iron-induced changes in the photosynthetic characteristics of sweet potato. J. Plant Physiol. 168, 2056–2062.

Adamski, J.M., Danieloski, R., Deuner, S., Braga, E.J.B., de Castro, L.A.S., Peters, J.A., 2012. Responses to excess iron in sweet potato: Impacts on growth, enzyme activities, mineral concentrations, and anatomy. Acta Physiol. Plant. 34, 1827–1836.

Araújo, T.O., Freitas-Silva, L., Santana, B.V.N., Kuki, K.N., Pereira, E.G., Azevedo, A.A., et al., 2014. Tolerance to iron accumulation and its effects on mineral composition and growth of two grass species. Environ. Sci. Pollut. R. 21, 2777–2784.

Barberon, M., Vermeer, J.E.M., De Bellis, D., Wang, P., Naseer, S., Andersen, T.G., et al., 2016. Adaptation of root function by nutrient-induced plasticity of endodermal differentiation. Cell 164, 447–459.

Becker, M., Asch, F., 2005. Iron toxicity in rice - Conditions and management concepts. J. Plant Nutr. Soil Sci. 168, 558–573.

Bilger, W., Björkman, O., 1990. Role of the xanthophyll cycle in photoprotection elucidated by measurements of light-induced absorbance changes, fluorescence and photosynthesis in leaves of *Hedera canariensis*. Photosynth. Res. 25, 173–185.

Briat, J.-F., Dubos, C., Gaymard, F., 2015. Iron nutrition, biomass production, and plant product quality. Trends Plant Sci. 20, 33–40.

Broadley, M., Brown, P., Çakmak, İ., Rengel, Z., Zhao, F., 2012. Function of Nutrients: Micronutrients. In: Marschner, P. (Ed.), Marschner's Mineral Nutrition of Higher Plants, 3rd ed. Academic Press, San Diego, pp. 191–248.

Celletti, S., Paolacci, A.R., Mimmo, T., Pii, Y., Cesco, S., Ciaffi, M., et al., 2016. The effect of excess sulfate supply on iron accumulation in three graminaceous plants at the early vegetative phase. Environ. Exp. Bot. 128, 31–38.

de la Fuente, C., Pardo, T., Alburquerque, J.A., Martínez-Alcalá, I., Bernal, M.P., Clemente, R., 2014. Assessment of native shrubs for stabilisation of a trace elements-polluted soil as the final phase of a restoration process. Agric. Ecosyst. Environ. 196, 103–111.

Deng, D., Wu, S.-C., Wu, F.-Y., Deng, H., Wong, M.-H., 2010. Effects of root anatomy and Fe plaque on arsenic uptake by rice seedlings grown in solution culture. Environ. Pollut. 158, 2589–2595.

Doblas, V.G., Geldner, N., Barberon, M., 2017. The endodermis, a tightly controlled barrier for nutrients. Curr. Opin. Plant Biol. 39, 136–143.

Evert, R.F., 2006. Structure and development of the plant body - an overview. In: Evert, R.F. (Ed.), Esau's Plant Anatomy: Meristems, Cells, and Tissues of the Plant Body - their Structure, Function, and Development, 3rd ed. John Wiley & Sons, Inc., New Jersey, pp. 1–13.

Genty, B., Briantais, J.M., Baker, N.R., 1989. The relationship between the quantum yield of photosynthetic electron transport and quenching of chlorophyll fluorescence. BBA-Gen. Subjects 990, 87–92.

Halliwell, B., 1987. Oxidative damage, lipid peroxidation and antioxidant protection in chloroplasts. Chem. Phys. Lipids 44, 327–340.

Hendrickson, L., Furbank, R.T., Chow, W.S., 2004. A simple alternative approach to assessing the fate of absorbed light energy using chlorophyll fluorescence. Photosynth. Res. 82, 73–81.

Hoagland, D.R., Arnon, D.I., 1950. The Water Culture Method for Growing Plants without Soil. California Agricultural Experiment Station, Berkeley, pp. 1–32.

Hodges, D.M., Delong, J.M., Forney, C.F., Prange, R.K., 1999. Improving the thiobarbituric-acid-reactive-substances assay for estimating lipid peroxidation in plant tissues containing anthocyanin and other interfering compounds. Planta 207, 604–611.

Huang, L., Li, W.C., Tam, N.F.Y., Ye, Z., 2018. Effects of root morphology and anatomy on cadmium uptake and translocation in rice (*Oryza sativa* L.). J. Environ. Sci. https://doi.org/10.1016/j.jes.2018.04.005.

Jucoski, G.O., Cambraia, J., Ribeiro, C., de Oliveira, J.A., de Paula, S.O., Oliva, M.A., 2013. Impact of iron toxicity on oxidative metabolism in young *Eugenia uniflora* L. plants. Acta Physiol. Plant. 35, 1645–1657.

Kobayashi, T., Nishizawa, N.K., 2012. Iron uptake, translocation, and regulation in higher plants. Annu. Rev. Plant Biol. 63, 131–152.

Kramer, D.M., Johnson, G., Kiirats, O., Edwards, G.E., 2004. New fluorescence parameters for the determination of Q_A redox state and excitation energy fluxes. Photosynth. Res. 79, 209–2018.

Li, W.C., Deng, H., Wong, M.H., 2017. Effects of Fe plaque and organic acids on metal uptake by wetland plants under drained and waterlogged conditions. Environ. Pollut. 231, 732–741.

Liu, H., Zhang, J., Christie, P., Zhang, F., 2008. Influence of iron plaque on uptake and accumulation of Cd by rice (Oryza sativa L.) seedlings grown in soil. Sci. Total Environ. 394, 361–368.

Lobréaux, S., Thoiron, S., Briat, J.F., 1995. Induction of ferritin synthesis in maize leaves by an iron mediated oxidative stress. Plant J. 8, 443–449.

Lyubenova, L., Pongrac, P., Vogel-Mikuš, K., Mezek, G.K., Vavpeti, P., Grlj, N., et al., 2012. Localization and quantification of Pb and nutrients in Typha latifolia by micro-PIXE. Metallomics 4, 333–341.

Melis, A., Spangfort, M., Andersson, B., 1987. Light absorption and electron transport balance between photosystem II and photosystem I in spinach chloroplasts. Photochem. Photobiol. 45, 129–136.

Michalak, A., 2006. Phenolic compounds and their antioxidant activity in plants growing under heavy metal stress. Pol. J. Environ. Stud. 15, 523–530.

Müller, C., Kuki, K.N., Pinheiro, D.T., de Souza, L.R., Siqueira-Silva, A.I., Loureiro, M.E., et al., 2015. Differential physiological responses in rice upon exposure to excess distinct iron forms. Plant Soil 391, 123–138.

Müller, C., Silveira, S.F.d.S., Daloso, D.d.M., Mendes, G.C., Merchant, A., Kuki, K.N., et al., 2017. Ecophysiological responses to excess iron in lowland and upland rice cultivars. Chemosphere 189, 123–133.

Murata, N., Takahashi, S., Nishiyama, Y., Allakhverdiev, S.I., 2007. Photoinhibition of photosystem II under environmental stress. BBA-Bioenergetics 1767, 414–421.

Oxborough, K., Baker, N.R., 1997. Resolving chlorophyll a fluorescence images of photosynthetic efficiency into photochemical and non-photochemical components – calculation of q_P and $F_v\text{-}/F_m\text{-}$; without measuring F_0. Photosynth. Res. 54, 135–142.

Pinto, S.S., de Souza, A.E., Oliva, M.A., Pereira, E.G., 2016. Oxidative damage and photosynthetic impairment in tropical rice cultivars upon exposure to excess iron. Sci. Agr. 73, 217–226.

Pugh, R.E., Dick, D.G., Fredeen, A.L., 2002. Heavy metal (Pb, Zn, Cd, Fe, and Cu) contents of plant foliage near the Anvil Range lead/zinc mine, Faro, Yukon Territory. Ecotox. Environ. Safe. 52, 273–279.

Redjala, T., Zelko, I., Sterckeman, T., Legué, V., Lux, A., 2011. Relationship between root structure and root cadmium uptake in maize. Environ. Exp. Bot. 71, 241–248.

Rios, C.O., Souza, B.C., Siqueira-Silva, A.I., Pereira, E.G., 2017. Assessment of iron toxicity in tropical grasses with potential for revegetation of mined areas. Pol. J. Environ. Stud. 26, 2167–2173.

Santana, B.V.N., de Araújo, T.O., Andrade, G.C., de Freitas-Silva, L., Kuki, K.N., Pereira, E.G., et al., 2014. Leaf morphoanatomy of species tolerant to excess iron and evaluation of their phytoextraction potential. Environ. Sci. Pollut. Res. 21, 2550–2562.

Schmidt, W., 2006. Iron stress responses in roots of strategy I plants. In: Barton, L.I., Abadia, J. (Eds.), Iron Nutrition in Plants and Rhizospheric Microorganisms. Springer, Dordrecht, pp. 229–250.

Sebastian, A., Prasad, M.N.V., 2016. Iron plaque decreases cadmium accumulation in Oryza sativa L. and serves as a source of iron. Plant Biol. 18, 1008–1015.

Silva, J.D.O.C., Paiva, E.A.S., Modolo, L.V., Nascentes, C.C., França, M.G.C., 2013. Removal of root apices enables study of direct toxic effects of aluminum on rice (Oryza sativa L.) leaf cells. Environ. Exp. Bot. 95, 41–49.

Silva, L., de Araújo, T., Martinez, C., de Almeida Lobo, F., Azevedo, A., Oliva, M., 2015. Differential responses of C_3 and CAM native Brazilian plant species to a SO_2- and SPMFe-contaminated Restinga. Environ. Sci. Pollut. Res. 22, 14007–14017.

Siqueira-Silva, A.I., Silva, L.C., Azevedo, A.A., Oliva, M.A., 2012. Iron plaque formation and morphoanatomy of roots from species of Restinga subjected to excess iron. Ecotox. Environ. Safe. 78, 265–275.

Sytar, O., Kumar, A., Latowski, D., Kuczynska, P., Strzałka, K., Prasad, M.N.V., 2013. Heavy metal-induced oxidative damage, defense reactions, and detoxification mechanisms in plants. Acta Physiol. Plant. 35, 985–999.

Tedesco, M.J., Gianello, C., Bissani, C.A., Bohnen, H., Volkweiss, S.J., 1995. Análise de solo, plantas e outros materiais. 2nd ed. Universidade Federal do Rio Grande do Sul, Porto Alegre, pp. 1–174.

Tylová, E., Pecková, E., Blascheová, Z., Soukup, A., 2017. Casparian bands and suberin lamellae in exodermis of lateral roots: an important trait of roots system response to abiotic stress factors. Ann. Bot. 120, 71–85.

Velikova, V., Yordanov, I., Edreva, A., 2000. Oxidative stress and some antioxidant systems in acid rain-treated bean plants: protective role of exogenous polyamines. Plant Sci. 151, 59–66.

Wang, X., Tam, N.F.-Y., He, H., Ye, Z., 2015. The role of root anatomy, organic acids and iron plaque on mercury accumulation in rice. Plant Soil 394, 301–313.

Wu, L.-B., Shhadi, M.Y., Gregorio, G., Matthus, E., Becker, M., Frei, M., 2014. Genetic and physiological analysis of tolerance to acute iron toxicity in rice. Rice 7, 1–12.

Wu, L.-B., Ueda, Y., Lai, S.-K., Frei, M., 2017. Shoot tolerance mechanisms to iron toxicity in rice (Oryza sativa L.). Plant Cell Environ. 40, 570–584.

Xu, S., Lin, D., Sun, H., Yang, X., Zhang, X., 2015. Excess iron alters the fatty acid composition of chloroplast membrane and decreases the photosynthesis rate: a study in hydroponic pea seedlings. Acta Physiol. Plant. 37, 1–9.

Yamaguchi, N., Mori, S., Baba, K., Kaburagi-Yada, S., Arao, T., Kitajima, N., et al., 2011. Cadmium distribution in the root tissues of solanaceous plants with contrasting root-to-shoot Cd translocation efficiencies. Environ. Exp. Bot. 71, 198–206.

Yousefi, Z., Kolahi, M., Majd, A., Jonoubi, P., 2018. Effect of cadmium on morphometric traits, antioxidant enzyme activity and phytochelatin synthase gene expression (SoPCS) of Saccharum officinarum var. cp48-103 in vitro. Ecotox. Environ. Safe. 157, 472–481.

Yuan, X., Guo, P., Qi, X., Ning, N., Wang, H., Wang, X., et al., 2013. Safety of herbicide Sigma Broad on Radix Isatidis (Isatis indigotica Fort.) seedlings and their photosynthetic physiological responses. Pestic. Biochem. Physiol. 106, 45–50.

Zhan, X., Zhu, M., Shen, Y., Yue, L., Li, J., Gardea-Torresdey, J.L., et al., 2018. Apoplastic and symplastic uptake of phenanthrene in wheat roots. Environ. Pollut. 233, 331–339.

Zhang, X., Zhang, F., Mao, D., 1999. Effect of iron plaque outside roots on nutrient uptake by rice (Oryza sativa L.): Phosphorus uptake. Plant Soil 209, 187–192.

Zhang, Y., Wang, Q., Xu, C., Sun, H., Wang, J., Li, L., 2016. Iron (Fe^{2+})-induced toxicity produces morphological and physiological changes in roots in Panax ginseng grown in hydroponics. Toxicol. Environ. Chem. 98, 630–637.